



¹⁴C PREPARATION PROTOCOLS FOR ARCHAEOLOGICAL SAMPLES AT THE LMC14, SACLAY, FRANCE

J-P Dumoulin¹  • C Moreau¹  • E Delqué-Količ¹ • I Caffy¹ • D Farcage² • C Goulas¹ • S Hain¹ • M Perron¹ • A Semerok² • M Sieudat¹ • B Thellier¹ • L Beck¹

¹Laboratoire de Mesure du Carbone 14 (LMC14), LSCE/IPSL, CEA-CNRS-UVSQ, Université Paris-Saclay, F-91191 Gif-sur-Yvette, France

²Université Paris-Saclay, CEA, Service d'Études Analytiques et de Réactivité des Surfaces, 91191 Gif-sur-Yvette, France

ABSTRACT. The Laboratoire de Mesure du Carbone 14 (LMC14) has operated a radiocarbon dating laboratory for almost twenty years with ARTEMIS, the Accelerator Mass Spectrometer (AMS) based on a NEC 9SDH-2 Pelletron tandem accelerator. A first status report describing the chemical pretreatment methods was published in 2017 (Dumoulin et al. 2017). This article summarizes updates of the routine procedures and presents new protocols. The quality checks in place at the LMC14 and results obtained for the GIRI international inter-comparison are reported. New protocols developed by the laboratory over the last five years are described with the preparation of iron, lead white, cellulose, calcium oxalate, and mortar. This report also provides a summary of practical information for sample preparation and can help the laboratory users who provide samples and publish results to better understand all the work behind a ¹⁴C dating.

KEYWORDS: archaeological samples, GIRI intercomparison, sample preparation protocols, status report.

INTRODUCTION

The Laboratoire de Mesure du Carbone 14 (LMC14) was established in 2003 in Saclay, France. This facility is a national laboratory and uses a 9SDH-2 Pelletron tandem accelerator from National Electrostatic Corporation (NEC). The accelerator mass spectrometer (AMS) ARTEMIS is dedicated to radiocarbon measurement and is funded by the following French research institutions: the Commissariat à l'Énergie Atomique et aux Énergies Alternatives (CEA), the Centre National de la Recherche Scientifique (CNRS), the Institut de Recherche pour le Développement (IRD), the Institut de Radioprotection et de Sûreté Nucléaire (IRSN), and the Ministère de la Culture (MC).

In 2023, the laboratory will celebrate its 20th anniversary and more than 70,000 samples of very different natures and origins will have been measured (Beck et al. 2023). In 2017, a status report explaining our protocols and laboratory procedures was published (Dumoulin et al. 2017). Over the last five years, “routine” protocols have continued to be applied on charcoals, wood or plant remains, shells, corals or foraminifera but also on artefacts containing various carbon contents such as paint, leather, wax or pearl. The quality of our procedures is often tested with international inter-comparison campaigns and the latest results for the GIRI inter-comparison are presented. More recently, new protocols have been developed to expand our range of datable materials and take into account the expectations of new archaeological projects. The specific protocols implemented for dating iron, cellulose (wood), calcium oxalates (rock art), mortars (buildings) or lead white (cosmetics and paintings) will be detailed.

SERVICE ACTIVITY: SAMPLE PREPARATION AND QUALITY CONTROL

As described in Dumoulin et al. (2017), for the service activity, two main types of samples are treated: carbonates and organic matter (OM). Carbonates include shell, coral, foraminifera,

*Corresponding author. Email: Jean-Pascal.Dumoulin@lsce.ipsl.fr

calcite crust or speleothems. After a microscope inspection and, if necessary, sand blasting, the samples are leached in a 10^{-2} N acid solution for 15 min. OM, including charcoals, wood, plants, peats and sediments are also subjected to microscopic examination to remove mineral grains and potential contaminants such as synthetic fibers or rootlets. Then, the samples are treated with the classical ABA method: acid (HCl, 0.5N, 80°C, 1 hr)—base (NaOH 0.1N, 80°C, 1 hr)—acid (HCl 0.5N, 80°C, 1 hr).

Sometimes, less common samples are dated in the laboratory with the same ABA protocol adapted according to the type, the fragility or the amount of the sample. This is the case for textile, rope, leather or paint and canvas (Beck et al. 2017; Quiles et al. 2021; Bonnot-Diconne et al. 2021; Beck 2022; Beck et al. 2022a). Some samples are directly combusted or hydrolysed without any pretreatment because the material is pure and was sampled directly inside the matrix; this is the case for pearls, amber or wax (Reiche et al. 2021; Beck et al. 2022b).

To control the efficiency of the pre-treatments as well as the quality of the measurements, the LMC14 participated in the last international intercomparisons SIRI (Scott et al. 2017; Moreau et al. 2020) and very recently GIRI. The LMC14 results for the GIRI are presented in Table 1.

The preparation and measurement of these GIRI samples, without knowing the consensus values in advance, was a very interesting challenge for the national laboratory. The presentation of the preliminary results at the Radiocarbon 24 International Conference in Zürich, Switzerland (Scott et al. [forthcoming](#)) makes it possible to assess the performance of the laboratory, and therefore the quality of the preparations and measurements carried out. A simple statistical test is used to evaluate each individual result: the z-score, defined as follows:

$$z = \frac{X_M - X_A}{\sigma_p}$$

where X_M is the reported result, X_A the assigned or true value for the sample and σ_p the target value for the standard deviation. Here the assigned value is the median calculated on the entire results given by the participating intercomparison laboratory and the quoted error is used for σ_p .

The interpretation of the z-score results is done as follows:

z-score = 0: it means a “perfect” result.

|z-score| ≤ 2: the single measurement result is “satisfactory”.

$2 < |z\text{-score}| < 3$: the single measurement result is still quite good but, “warning”, the agreement between the result with its error and the consensus value begins to be less good.

|z-score| ≥ 3: this would be a very unusual result and further “investigation” would be needed to find out the reason for the discrepancy.

The results of the GIRI sample prepared and blindly measured on the LMC14 ARTEMIS AMS facility show excellent agreement with the preliminary consensus values of each sample. The z-score values are, with the exception of one case out of the 51 results, less than 2, which means “satisfactory”. These results show the excellent performance of the LMC14 in C14 analysis.

Table 1 LMC14 GIRI results. In this table, the values are not rounded as is the usual practice with radiocarbon results. F_m is the fraction modern of the sample background corrected. Results not distinguishable from the background are indicated as < in Fraction modern (F_m) and > in Before Present (BP).

GIRI Sample code	LMC14 Sample reference	$\delta^{13}C \pm 1\sigma$ error (permil)	F_m value $\pm 1\sigma$ error	Age $\pm 1\sigma$ error (BP)	Age limit	LMC14 F_m Mean value $\pm 1\sigma$ error	z-score	z-score interpretation
A	SacA 65972	-25.9 ± 0.5	1.16185 ± 0.00445			1.16367 ± 0.00337	-0.75	Satisfactory
A	SacA 65973	-25.5 ± 0.4	1.16891 ± 0.00440				0.84	Satisfactory
A	SacA 65974	-21.1 ± 0.5	1.16058 ± 0.00425				-1.09	Satisfactory
A	SacA 66566	-24.8 ± 0.2	1.16507 ± 0.00436				-0.03	Satisfactory
A	SacA 66567	-25.2 ± 0.3	1.16194 ± 0.00422				-0.77	Satisfactory
B	SacA 65975	-28.5 ± 0.3	0.22985 ± 0.00110	11811 ± 38		0.22892 ± 0.00100	0.03	Satisfactory
B	SacA 65976	-26.3 ± 0.6	0.22906 ± 0.00108	11839 ± 38			0.76	Satisfactory
B	SacA 65977	-29.6 ± 0.6	0.22785 ± 0.00124	11881 ± 44			1.61	Satisfactory
C	SacA 65978	-34.0 ± 0.3	1.02391 ± 0.00371			1.02424 ± 0.00053	0.38	Satisfactory
C	SacA 65979	-32.4 ± 0.3	1.02396 ± 0.00380				0.38	Satisfactory
C	SacA 65980	-32.6 ± 0.4	1.02485 ± 0.00381				0.62	Satisfactory
D	SacA 65981	-31.3 ± 0.4	0.62401 ± 0.00195	3788 ± 30		0.62419 ± 0.00127	-1.02	Satisfactory
D	SacA 65982	-29.7 ± 0.4	0.62303 ± 0.00172	3801 ± 30			-0.58	Satisfactory
D	SacA 65983	-29.3 ± 0.4	0.62555 ± 0.00180	3768 ± 30			-1.68	Satisfactory
E	SacA 65984	-32.8 ± 0.6	0.95250 ± 0.00242	391 ± 30		0.95379 ± 0.00360	0.37	Satisfactory
E	SacA 65985	-27.6 ± 0.4	0.95794 ± 0.00188	345 ± 30			-1.17	Satisfactory
E	SacA 65986	-28.2 ± 0.4	0.95687 ± 0.00184	354 ± 30			-0.87	Satisfactory
E	SacA 66568	-25.8 ± 0.2	0.95253 ± 0.00201	391 ± 30			0.37	Satisfactory
E	SacA 66569	-24.8 ± 0.3	0.94911 ± 0.00212	420 ± 30			1.33	Satisfactory
F	SacA 65987	-28.4 ± 0.2	1.00842 ± 0.00380			1.01236 ± 0.00528	-1.89	Satisfactory
F	SacA 65988	-25.9 ± 0.3	1.00509 ± 0.00368				-2.86	Warning
F	SacA 65989	-28.4 ± 0.4	1.01611 ± 0.00375				0.14	Satisfactory
F	SacA 66570	-27.9 ± 0.3	1.01682 ± 0.00384				0.32	Satisfactory
F	SacA 66571	-27.6 ± 0.3	1.01535 ± 0.00380				-0.07	Satisfactory
G	SacA 65990	-24.3 ± 0.3	0.56755 ± 0.00145	4550 ± 30		0.56824 ± 0.00063	0.80	Satisfactory
G	SacA 65991	-24.3 ± 0.3	0.56880 ± 0.00158	4532 ± 30			0.20	Satisfactory
G	SacA 65992	-24.7 ± 0.3	0.56836 ± 0.00148	4539 ± 30			0.43	Satisfactory

(Continued)

Table 1 (*Continued*)

GIRI Sample code	LMC14 Sample reference	$\delta^{13}\text{C} \pm 1\sigma$ error (permil)	Fm value $\pm 1\sigma$ error	Age $\pm 1\sigma$ error (BP)	Age limit	LMC14 Fm Mean value $\pm 1\sigma$ error	z-score	z-score interpretation
HB	SacA 65993	-20.6 ± 0.5	0.75828 ± 0.00183	2223 ± 30		0.75047 ± 0.00139	0.73	Satisfactory
HB	SacA 65994	-21.0 ± 0.3	0.75912 ± 0.00170	2214 ± 30			0.43	Satisfactory
HB	SacA 65995	-21.5 ± 0.3	0.76099 ± 0.00166	2194 ± 30			-0.23	Satisfactory
I	SacA 65996	-22.7 ± 0.2	0.05218 ± 0.00083	23722 ± 128		0.05162 ± 0.00056	0.49	Satisfactory
I	SacA 65997	-23.0 ± 0.3	0.05105 ± 0.00083	23897 ± 131			1.82	Satisfactory
I	SacA 65998	-22.5 ± 0.4	0.05163 ± 0.00083	23807 ± 129			1.15	Satisfactory
J	SacA 65999	-26.0 ± 0.3	0.00705 ± 0.00077	39804 ± 877		0.00715 ± 0.00026	1.35	Satisfactory
J	SacA 66000	-26.0 ± 0.3	0.00745 ± 0.00077	39363 ± 835			0.89	Satisfactory
J	SacA 66001	-23.8 ± 0.5	0.00697 ± 0.00077	39894 ± 888			1.44	Satisfactory
LB	SacA 66002	-22.4 ± 0.5	0.75756 ± 0.00168	2230 ± 30		0.75678 ± 0.00071	-0.23	Satisfactory
LB	SacA 66003	-20.0 ± 0.4	0.75619 ± 0.00175	2245 ± 30			0.27	Satisfactory
LB	SacA 66004	-22.6 ± 0.4	0.75658 ± 0.00167	2241 ± 30			0.13	Satisfactory
M	SacA 66005	-27.1 ± 0.3	0.98549 ± 0.00194	117 ± 30		0.98664 ± 0.00100	-0.47	Satisfactory
M	SacA 66006	-25.5 ± 0.4	0.98710 ± 0.00196	104 ± 30			-0.91	Satisfactory
M	SacA 66007	-27.5 ± 0.3	0.98732 ± 0.00191	103 ± 30			-0.94	Satisfactory
N	SacA 66008	-20.5 ± 0.4	< 0.00190	Not distinguishable	> 50318	0.00186 ± 0.00015		
N	SacA 66009	-23.0 ± 0.4	< 0.00169	Not distinguishable	> 51254			
N	SacA 66010	-20.0 ± 0.4	< 0.00198	Not distinguishable	> 49993			
O	SacA 66011	-30.2 ± 0.3	0.22811 ± 0.00113	11872 ± 40		0.22869 ± 0.00051	1.38	Satisfactory
O	SacA 66012	-28.8 ± 0.4	0.22898 ± 0.00117	11841 ± 41			0.59	Satisfactory
O	SacA 66013	-27.1 ± 0.5	0.22899 ± 0.00115	11841 ± 40			0.60	Satisfactory
P	SacA 66014	-25.4 ± 0.4	0.75392 ± 0.00181	2269 ± 30		0.75361 ± 0.00120	1.12	Satisfactory
P	SacA 66015	-22.4 ± 0.4	0.75462 ± 0.00191	2262 ± 30			0.88	Satisfactory
P	SacA 66016	-23.7 ± 0.4	0.75228 ± 0.00173	2287 ± 30			1.72	Satisfactory
Q	SacA 66017	-25.2 ± 0.4	0.95446 ± 0.00194	374 ± 30		0.95592 ± 0.00336	1.23	Satisfactory
Q	SacA 66018	-23.8 ± 0.5	0.95353 ± 0.00188	382 ± 30			1.50	Satisfactory
Q	SacA 66019	-25.3 ± 0.3	0.95975 ± 0.00185	330 ± 30			-0.23	Satisfactory

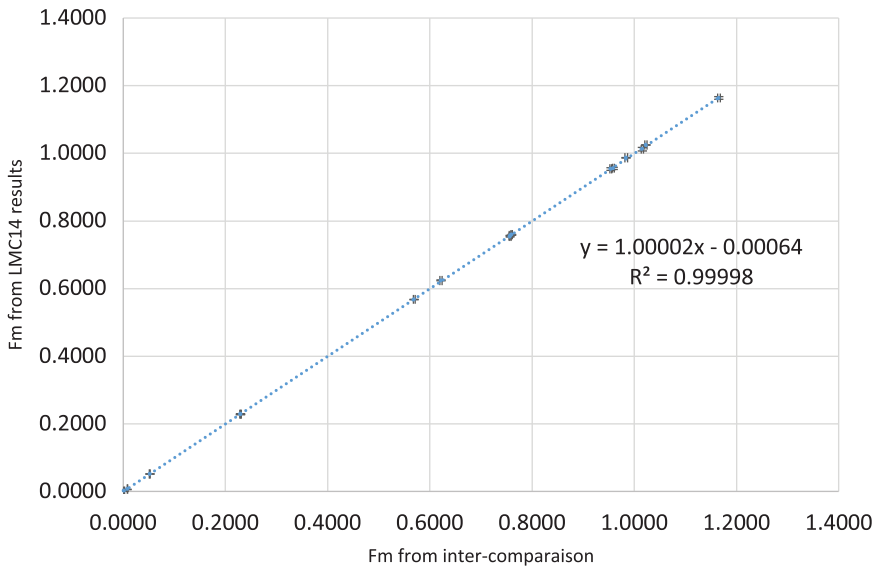


Figure 1 Linear regression on the F_m data coming from the intercomparison and the LMC14 results (mean per sample).

Figure 1 presents the average of the measurements in fraction modern for each of the GIRIs according to the associated preliminary results in F_m (median of the values provided by the participating international laboratories), coupled with their respective error bars, over the entire time range reachable by ^{14}C analysis.

By performing a linear fit on these points (consensus value in F_m ; mean of experimental results in F_m), a linear regression curve on plot 1 is obtained:

$$F_{m \text{ exp result}} = a \cdot F_{m \text{ consensus value}} + b$$

with

Leading coefficient: $a = 1.00002$

y-intercept: $b = -0.00064$

Square of the correlation coefficient: $R^2 = 0.99998$

The leading coefficient is equal to 1, to within 2×10^{-5} . The y-intercept is close to zero and is a negative value. It depends on the measured background level, which is greater than the consensus value in this case. The correlation coefficient calculated from Pearson's correlation formula is very close to 1, to within 2×10^{-5} , showing that there is no significant difference between the experimental results and the associated consensus values over the entire time domain accessible by radiocarbon analysis.

NEW DEVELOPMENTS FOR SAMPLE PREPARATION

Beside our service activity for the French scientific community, the laboratory develops new protocols to widen the range of the datable materials and to respond to various challenges raised in the context of different scientific collaborations.

Iron Objects

As tools, weapons or elements of architecture, iron objects are critical markers of societies development for more than 3000 years. Until the beginning of the nineteenth century, iron was produced from the reduction of iron ore by carbon oxide provided by the combustion of wood charcoal. Carbon was trapped into the metallic matrix in the form of iron carbide with a ^{14}C content derived from the wood charcoal used as fuel in the reduction process. In these conditions, iron objects are suitable for direct radiocarbon dating. A specific methodology to prepare samples taken from massive iron objects was developed in collaboration with the Laboratoire Archéomatériaux et Prévision de l'Altération (CEA-CNRS, Saclay, France) (Leroy et al. 2015). Prior to ^{14}C dating, a metallographic study is performed on a cross-section of the metal to inform on its micro-structure and avoid any risks of misdating that could be due to the recycling process or to exogenous carbon. Then, sampling is done by drilling in the most carburized areas of the cross-section that were determined by the metallographic observation. However, when the iron piece is located within the object, as in the case of some bronze statues reinforced with iron armatures, sampling is only possible by drilling the exposed part of the armature directly (Leroy et al. 2021). Careful observation is necessary to select the most appropriate part and avoid any damage to the artwork. Before drilling, the surface is sanded down with a grinding wheel until the metallic surface is exposed and possible contamination eliminated. The iron particles are then combusted at 850°C for 5 hr in an excess of CuO and a 1 cm pure Ag wire (Dumoulin et al. 2017).

Another sampling protocol for iron alloys is being experimented with a laser beam. In the literature, this technique is used for isotopic analysis of tooth enamel and shells (Rosenheim et al. 2008; Garcia et al. 2015) and was also tested for ^{14}C dating of organic matter by Watchman et al. (1992). This method offers two advantages: the precision of sampling due to the sharp beam that can be computer-monitored, and the one-step production of CO_2 that limits sample handling and consequently avoids possible contamination. A first experiment was carried out to test the feasibility of this sampling procedure on a cast iron sample GL03-24 (2–3% C) coming from an iron-making archaeological site—the Glinet site—whose operation is attested between 1480 and 1580 AD by historical texts (Arribet-Deroin 2001; Leroy et al. 2015). This iron piece was selected because of its homogeneous and high carbon content that are more suitable for an initial experiment with the laser beam. The laser beam was produced by an ytterbium pulsed fiber laser which provides a wavelength output at around 1064 nm (YLP-V2 1mJ series from IPG Laser) and operates at 20 W with 140 ns temporal width. A cross section was prepared and enclosed in a cell pumped until 10^{-5} mbar and filled with 250 mbar of pure oxygen. A 4.5 cm^2 area was scanned by the laser beam for 8 hr and 4.6 mg of carbon in the form of CO_2 was recovered for graphitization on the automated graphitization line (Dumoulin et al. 2017). Two dates were obtained (Table 2)— 360 ± 30 BP and 345 ± 30 BP—that gave a calibrated range between the middle of the 15th century and the middle of the 17th century, in perfect agreement with the expected period of metallurgical activity of the Glinet metallurgical site. These initial results suggest several possibilities for improvement. In particular, the laser ablation parameters need to be optimized to increase the carbon extraction yield and its oxidation in CO_2 .

Table 2 ^{14}C dates obtained on archaeological cast iron after collecting CO_2 by laser ablation. The results are in agreement with the expected range of dates 1480–1580 AD.

Sample	Lab ID	mg C	$\delta^{13}\text{C}$ ‰	BP age	Calibrated range at 95.4%
GL03-24	SacA 56907	1.76	−27.5	360 ± 30	1450 AD–1635 AD
	SacA 56908	1.63	−29.8	345 ± 30	1465 AD–1638 AD

Lead White Used as Cosmetic and Pigment

Lead white was one of the most important pigments used for more than 25 centuries. This pigment, composed of cerussite, (PbCO_3) and hydrocerussite, ($\text{Pb}_3(\text{CO}_3)_2(\text{OH})_2$) occurs in nature but was also manufactured from the 4th–3rd centuries BC to the early 20th century. During this long period, and until the 19th century, lead white was synthesized by corrosion, involving lead, vinegar and a fermenting medium (such as horse manure). Then, new industrial processes using fossil sources of CO_2 were developed to produce large amounts of lead white. Synthetic lead carbonates have been shown to carry the carbon isotopic signature of the initial ingredients (Messenger et al. 2022; Beck et al. 2023 in this collection) leading to a possible absolute dating of lead white by ^{14}C when all the ingredients participating in its synthesis are of organic origin. This hypothesis has been confirmed by the successful radiocarbon dating of Greek cosmetics (Beck et al. 2018), Roman collyria (Messenger et al. 2021), pigment (Messenger et al. 2022) and paint (Beck et al. 2018; Messenger et al. 2019; Hendriks et al. 2019, 2020b; Beck et al. 2020). On the contrary, when lead carbonates are produced using a fossil source of CO_2 , absolute dating is not possible. However, the absence of ^{14}C allows the identification of modern productions that are therefore indirectly dated (Messenger et al. 2022).

To prepare carbonate samples for radiocarbon analysis, acid hydrolysis is usually performed. However, this procedure is not carbonate selective in the case of a mixture of lead white and calcite, which is very common in paintings. In order to avoid contamination by dead carbon from calcite, the thermal decomposition approach was investigated, showing that heating the sample to 400°C leads to the release of CO_2 from lead carbonate only when mixed with calcite (Beck et al. 2019). However, when lead white and linseed oil are mixed to form a paint layer, part of the linseed oil also decomposes at 400°C (Messenger et al. 2020). The proportion of linseed oil extracted during the thermal preparation contributes to the radiocarbon dating of the paint layer together with lead white. If the two ingredients are contemporaneous, the partial decomposition of the binder does not alter the date obtained from lead white. In the case of acrylic-based paints, however, the small quantity of CO_2 extracted will give an incorrect apparent age. To overcome this issue, it is necessary to decrease the heating temperature to 250°C–300°C as also pointed out by Hendriks et al. (2020a) for paint reconstructions prepared with linseed oil, lead carbonate and calcium carbonate. In conclusion, it is important to chemically characterize the paint layer before ^{14}C dating to adjust the decomposition temperature.

Calcium Oxalates

Dating rock paintings is difficult as the carbon content of the paint layers is tiny or sometimes non-existent. The ^{14}C dating of calcium oxalate deposits covering the rock paintings can then provide a limit, a *terminus ante quem* for the age of the rock art. A technique was tested for the chemical extraction of oxalates (Figure 2) from the mineral crust taken from decorated walls in Namibia (Erongo Massif).

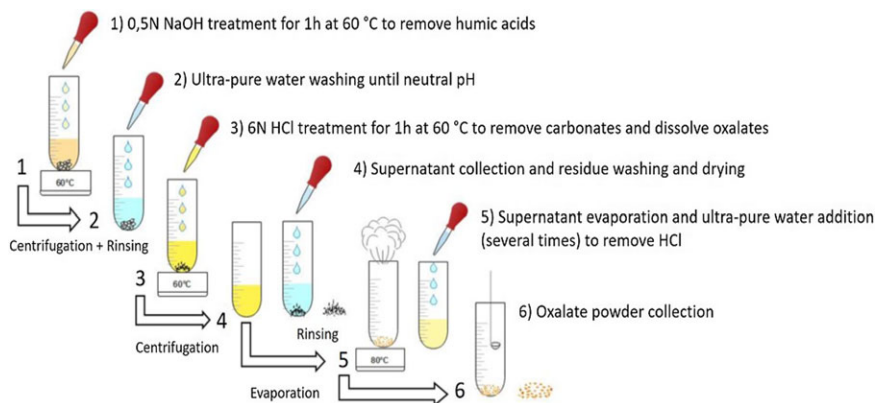


Figure 2 Protocol for calcium oxalate extraction developed at the LMC14 (from Dumoulin et al. 2020).

The powdered material (between 200 and 400 mg) was introduced in a NaOH solution (0.5N) at 60°C for 1 hr to remove humic acids. After extensive rinsing with Milli-Q[®] water, the sample was treated with 6N HCl at 60°C, to remove carbonates and to dissolve the calcium oxalates and in particular the whewellite ($\text{CaC}_2\text{O}_4 \cdot \text{H}_2\text{O}$) and the weddellite ($\text{CaC}_2\text{O}_4 \cdot 2\text{H}_2\text{O}$). After 1 hr, the solution was centrifuged and the supernatant was decanted and saved. The precipitate, called “residue”, which contain various solids such as silica, pollen, charcoal or windblown material was removed. The supernatant containing oxalic and HCl acids was evaporated, washed with ultra-pure water and evaporated several times to remove a maximum of HCl with the evaporation. It avoids having strong acid fumes during combustion which can weaken and break the quartz tube.

Oxalate and the organic residues of the crusts were successfully separated and the different fractions were ¹⁴C dated. FTIR was used to monitor the different pre-treatment phases ranging from raw samples to pure oxalates as well as their organic residues. This preliminary technical study allowed us to define a robust and reliable protocol for oxalate extraction (Jones et al. 2017; Dumoulin et al. 2020)

Cellulose Extraction

After the catastrophic fire of Notre Dame de Paris cathedral in 2019, several multidisciplinary working groups drew up a plan to study the building materials: stone, metal and wood. Our laboratory takes part in the CASIMODO national research project to refine the ¹⁴C calibration curve around the 12th century by comparing dendrochronological analyses of the wooden frame (oak) with ¹⁴C dating of cellulose tree rings (Daux et al. 2022).

The main components of wood are cellulose (40–60%), lignin (16–33%), hemicelluloses and easily extractable minor components (5–10%), such as resins or waxes. The relative component ratios depend on the type of tree and wood species (Němec et al. 2010). Cellulose is a long-chain carbon-based glucan polymer (Leavitt and Danzer 1993) with a very stable molecular formula $(\text{C}_6\text{H}_{10}\text{O}_5)_n$. Cellulose remains unchanged and immobile over long periods of time, representing the isotopic composition of the original plant material, while lignin and hemicelluloses are considered susceptible to longer-term change. The carbon of these compounds can cross the boundaries of tree

rings after their formation (Wilson and Grinstead 1977; Leavitt and Danzer 1993; Gaudinski et al. 2005). Cellulose and hemicelluloses are collectively called holocellulose.

There are a large number of different treatments for the extraction of cellulose and they can depend considerably on the types of wood. Capano et al. (2018) compared several protocols, two of which were selected for this study: the BABA-B (Base/Acid/Base/Acid/Bleaching) protocol, developed by Němec et al. (2010) and the ABA-B protocol proposed by Capano et al. (2018). Some other protocols recommend eliminating the hemicellulose with a final step of sodium hydroxide (NaOH, 17.5%) to leave only the insoluble α -cellulose. The advisability of this final step is not agreed upon by all researchers and some consider it as a too destructive chemical treatment when the wood is old and poorly preserved. Furthermore, the study published in 2014 by Richard et al. showed that some tree species, such as oak and beech, did not need the NaOH treatment and a less intensive chemical procedure can actually lead to pure α -cellulose.

The tree ring samples are cut into small wood chips using a scalpel. An intercomparison sample of oak called FIRI H (*Quercus robur*) was prepared. The BABA-B protocol (Němec et al. 2010) consists in leaving the samples in a bath of 5 mL of 4% NaOH at 75°C overnight (16 hr) to dissociate the alcoholic, phenolic and carboxylic groups of the main components of wood. Cellulose is then more accessible for subsequent treatments. The next day, ABA procedures are performed and samples are placed on a heat block at 75°C. A treatment with 4% HCl (5 mL) is carried out for 1 hr to eliminate the contamination of carbonates followed by a bath of 4% NaOH (5 mL) for 1 hr and a second step of 4% HCl (5 mL) for 1 hr to remove any absorbed atmospheric CO₂. Finally, a bleach solution (8 g of NaClO₂ with 300 mL of ultrapure water and 11 ml of 37% HCl) to remove lignin and other contaminants is applied for 2 hr and can be repeated if needed. The final extract is dried in an oven at 55°C overnight. The ABA-B treatment (Capano et al. 2018) is the same without the NaOH bath overnight. In our study we compared different treatment times to determine an optimised protocol for oak wood.

The quality of our extractions is controlled by Fourier transform infrared spectroscopy (FTIR) in attenuated total reflectance mode (ATR-FTIR). This allows the identification of the characteristic bands of the different compounds present in the wood. The spectrum of raw oak wood (FIRI H without pretreatment) was carried out in order to associate each absorption band with its component. Different characteristic bands appeared from the three main constituents of wood, namely cellulose, hemicelluloses and lignin, and were attributed according to the literature (Figure 3; Rinne et al. 2005; Antchukaitis et al. 2008; Fogtman-Schulz et al. 2020). In order to monitor the effectiveness of the protocols, the absence of the lignin band (1508 cm⁻¹) and hemicellulose band (1732 cm⁻¹) was checked (Figure 3).

The spectra in Figure 3 show that for the FIRI H, the ABA-bleaching 2 hr is enough to remove the lignin and most of the hemicellulose. There is no need to apply a 4% NaOH bath at 75°C overnight (16 hr). It also confirms that the bleaching step is very important to remove lignin, which is still present with ABA or B(16h)-ABA treatments.

Then, the dating of three different wood samples (SIRI G, FIRI H and a wood background sample) was performed after an ABA-Bleaching 2 hr pretreatment. The results (Table 3) are in accordance with the consensual values within 1 σ error (Scott 2003; Scott et al. 2017).

The ABA-B procedure was chosen based on its accurate measurements on different ancient and blank wood samples. The treatment proposed by Capano et al. (2018) presents many

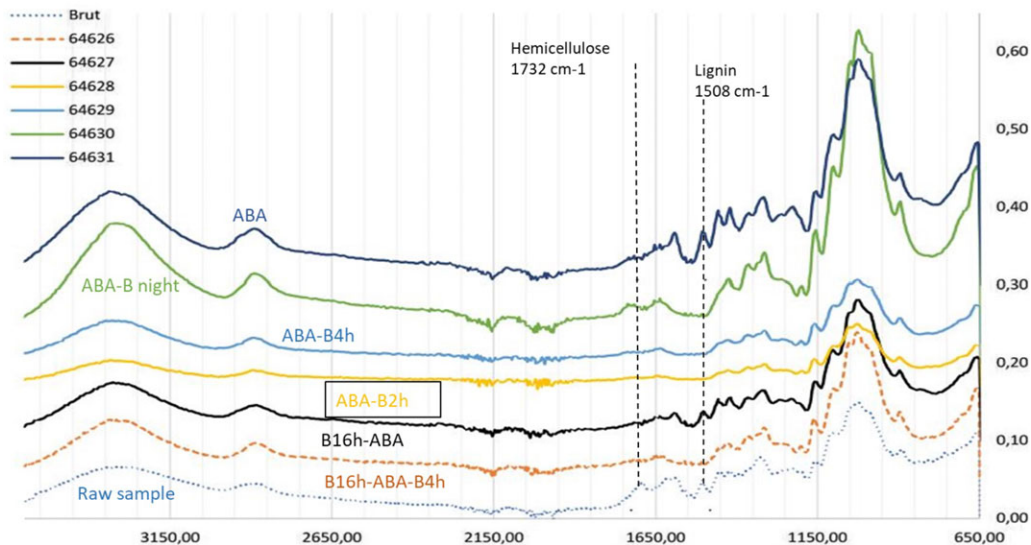


Figure 3 FTIR spectra of FIRI H oak sample according to the pretreatment procedure (ABA, ABA-Bleaching overnight, ABA-bleaching 4 hr, ABA-bleaching 2 hr, B16h-ABA-bleaching 4 hr, B16h-ABA-no bleaching). Raw FIRI H without any treatment shows a lignin band at 1508 cm⁻¹ and a hemicellulose band at 1732 cm⁻¹.

Table 3 ¹⁴C measurements of three samples (SIRI G, FIRI H and a wood background sample).

Sample	Lab ID	mg C	$\delta^{13}\text{C}$ ‰	pMC	BP age	Consensual value BP
SIRI G (ABA-B)	SacA 65100	1.05	-24.4	95.046 ± 0.246	410 ± 30	377 ± 3
FIRI H (ABA-B)	SacA 64628	1.06	-24.0	75.514	2255 ± 30	2232 ± 5
Chiloé (ABA-B)	SacA 65102	1.42	-32.0	0.164 ± 0.01	51490 ± 500	Background sample

advantages: the overall duration is shorter than that of other procedures, the protocol is not too destructive in the case of small wood samples, and it removes lignin and a large part of hemicellulose. These treatments omit the post-bleaching bath in base solution (NaOH 17%) which does not appear to be necessary for oak wood.

Mortar

The ¹⁴C dating of mortars is a real challenge because the contaminants are of the same nature (CaCO₃) as the sample itself. The idea is to date the atmospheric CO₂ trapped during the hardening of the binder and which re-carbonated the lime mortar. However, recrystallization, delayed hardening, layered double hydroxide compounds (LDH), fire damage as well as geological carbonate can strongly disturb the dating (Labeyrie and Delibrias 1964; Stuiver and Smith 1965; Heinemeier et al. 1997; Lindroos et al 2012; Ricci et al. 2020). In the framework of MODIS2 (Mortar Dating Inter-comparison Study number 2), the LMC14 proposed a

Table 4 LMC14 results for three MODIS2 mortar samples and preliminary results of the other laboratories with the range of results and the median value. Several Id. Lab labels are shown for each sample, corresponding to the different temperature experiments necessary to determine the plateau zone of ^{14}C .

Sample	Lab ID	LMC14 results (plateau BP ages)	Preliminary consensual values (BP) from different Laboratories [range], median
MODIS2-1	SacA 64898 to SacA 64904	693 ± 22	[484–767], median 634
MODIS2-2	SacA 64905 to SacA 64910	689 ± 22	[602–899], median 682
MODIS2-3	SacA 64911 to SacA 64920	1874 ± 30	[1680–2024], median 1802

preparation protocol based on the extraction of CO_2 by thermal decomposition. This protocol was coupled to a preliminary study, carried out by a thermal gravimetric analysis (TGA), which made it possible to select the appropriate extraction temperatures (Moreau et al. [forthcoming](#)).

The mortar was gently crushed with pliers to avoid producing small grains of geological carbonates which can contaminate the lime mortar (Heinemeier et al. [2010](#)). Sieves $< 100 \mu\text{m}$ were used to collect the under $100 \mu\text{m}$ fraction of the powder. The sample was then characterized by TGA to determine the range of temperatures to be applied to release and collect the different CO_2 fractions.

An amount of 200 mg of this $<100 \mu\text{m}$ mortar powder was placed in a quartz tube with quartz wool (previously cleaned at 900°C overnight) to prevent the sample from being sucked into the vacuum line. The mortar powder was pre-heated at 550°C for half an hour to remove organic contaminants and layered double hydroxide (LDH) which can introduce young carbon dioxide (Ricci et al. [2020](#); Daugbjerg et al. [2021](#)).

The preheating and the heating of the mortar were carried out on the same vacuum line. A succession of different temperature intervals (every $20\text{--}30^\circ\text{C}$) was applied and different fractions were collected to cover the working range determined by TGA. Each sample was graphitized and measured using the ARTEMIS facility (Dumoulin et al. [2017](#); Moreau et al. [2020](#)). By comparing the different radiocarbon measurements, the aim was to locate a plateau corresponding to the CO_2 release of lime mortar, before a dip and an aging created by the release of geological limestone. The correct age of the mortar should be located in this plateau.

The definitive results for the MODIS2 intercomparison will be presented in a later article (Scott et al. [forthcoming](#)) but a summary of our results compared to the preliminary results of the laboratories participating to the intercomparison is presented in Table 4. More details can be found in this proceedings (Moreau et al. [forthcoming](#)).

CONCLUSION

The last overview of the chemical pretreatment procedures for LMC14 ^{14}C dating was published in 2017 (Dumoulin et al. [2017](#)) and these protocols still give very good results as show the results of last GIRI international intercomparison. While the routine procedures remain the same, new ones have been added to widen our range of datable materials. The studies

undertaken by the LMC14 are the result both of collaboration with outside researchers and of active research by the members of the laboratory itself. In the coming years, all the LMC14 team will continue its efforts to address new challenges in ^{14}C dating and to support the French scientific community in different fields and especially in archaeology.

ACKNOWLEDGMENTS

The authors thank Stéphanie Leroy and Enrique Vega from the Laboratoire Archéomatériaux et Prédiction de l'Altération (IRAMAT UMR5060 CNRS et NIMBE UMR3685 CEA/CNRS) for their advice and assistance during the iron sample preparation for laser experiment and Maguy Jaber from the LAMS (Sorbonne Université) for the TGA experiments.

REFERENCES

- Arribet-Deroin D. 2001. Fondre le fer en gueuses au XVI^e siècle. Le haut fourneau de Glinet en pays de Bray (Normandie) [PhD thesis in Archaeology]. Paris I Sorbonne, Paris.
- Anchukaitis KJ, Evans MN, Lange T, Smith DR, Leavitt SW, Schrag DP. 2008. Consequences of a Rapid Cellulose Extraction Technique for Oxygen Isotope and Radiocarbon Analyses. *Analytical Chemistry* 80(6):2035–2041. doi: [10.1021/ac7020272](https://doi.org/10.1021/ac7020272)
- Beck L. 2022. Ion beam analysis and ^{14}C accelerator mass spectroscopy to identify ancient and recent art forgeries. *Physics* 4(2):462–472. doi: [10.3390/physics4020031](https://doi.org/10.3390/physics4020031)
- Beck L et al. 2018. Absolute dating of lead carbonates in ancient cosmetics by radiocarbon. *Communications Chemistry* 1(1):1–7. doi: [10.1038/s42004-018-0034-y](https://doi.org/10.1038/s42004-018-0034-y).
- Beck L et al. 2022a. Detecting recent forgeries of Impressionist and Pointillist paintings with high-precision radiocarbon dating. *Forensic Science International* 333:111214. doi: [10.1016/j.forsciint.2022.111214](https://doi.org/10.1016/j.forsciint.2022.111214).
- Beck L et al. 2022b. Marine reservoir effect of spermaceti, a wax obtained from the head of the sperm whale: a first estimation from museum specimens. *Radiocarbon* 64(6):1607–1616. doi: [10.1017/RDC.2022.79](https://doi.org/10.1017/RDC.2022.79)
- Beck L, Alloin E, Vigneron A, Caffy I, Klein U. 2017. Ion beam analysis and AMS dating of the silver coin hoard of Preuschorf (Alsace, France). *Nuclear Instruments and Methods in Physics Research B* 406:93–98. doi: [10.1016/j.nimb.2017.01.008](https://doi.org/10.1016/j.nimb.2017.01.008)
- Beck L, Caffy I, Delqué-Količ E, Dumoulin J-P, Goulas C, Hain S, et al. 2023. 20 years of AMS ^{14}C dating using the ARTEMIS facility at the LMC14 National Laboratory: review of service and research activities. *Radiocarbon*. doi: [10.1017/RDC.2023.23](https://doi.org/10.1017/RDC.2023.23)
- Beck L, Messenger C, Caffy I, Delqué-Količ E, Perron M, Dumoulin J-P, et al. 2020. Unexpected presence of ^{14}C in inorganic pigment for an absolute dating of paintings. *Scientific reports* 10:9582. doi: [10.1038/s41598-020-65929-7](https://doi.org/10.1038/s41598-020-65929-7).
- Beck L, Messenger C, Coelho S, Caffy I, Delqué-Količ E, Perron M, et al. 2019. Thermal decomposition of lead white for radiocarbon dating of paintings. *Radiocarbon* 61(5):1345–1356. doi: [10.1017/RDC.2019.64](https://doi.org/10.1017/RDC.2019.64)
- Bonnot-Diconne et al. 2021. La datation des cuirs dorés : confirmer et affiner la chronologie d'un objet d'art décoratif ? *Techné* 52:68–74. doi: [10.4000/techné.9969](https://doi.org/10.4000/techné.9969)
- Capano M, Miramont C, Guibal F, Kromer B, Tuna T, Fagault Y, Bard E. 2018. Wood ^{14}C dating with AixMICADAS: methods and application to tree-ring sequences from the Younger Dryas Event in the southern French Alps. *Radiocarbon* 60(1):51–74. doi: [10.1017/rdc.2017.83](https://doi.org/10.1017/rdc.2017.83)
- Daugbjerg T, Lindroos A, Hajdas I, Ringbom A, Olsen J. 2021. Comparison of thermal decomposition and sequential dissolution—two sample preparation methods for radiocarbon dating of lime Mortars. *Radiocarbon* 63. doi: [10.1017/RDC.2020.144x](https://doi.org/10.1017/RDC.2020.144x)
- Daux et al. 2022. The “forest” of Notre-Dame de Paris: a possible path into medieval climate and time. *Journal of Cultural Heritage*. doi: [10.1016/j.culher.2022.09.002](https://doi.org/10.1016/j.culher.2022.09.002)
- Dumoulin JP, Comby-Zerbino C, Delqué-Količ E, Moreau C, Caffy I, Hain S, et al. 2017. Status report on sample preparation protocols developed at the LMC14 Laboratory, Saclay, France: from sample collection to ^{14}C AMS measurement. *Radiocarbon* 59:713–726.
- Dumoulin JP, Lebon M, Caffy I, Mauran G, Nankela A, Pleurdeau D, Beck L. 2020. Calcium oxalate radiocarbon dating: preliminary tests to date rock art of decorated open-air caves of Erongo Mountains in Namibia. *Radiocarbon*, 1–12. Doi:[10.1017/RDC.2020.81](https://doi.org/10.1017/RDC.2020.81)
- Fogtmann-Schulz A, Kudsk SGK, Adolphi F, Karoff C, Knudsen MF, Loader NJ, et al. 2020. Batch processing of tree-ring samples for radiocarbon analysis. *Radiocarbon* 1–13. doi: [10.1017/rdc.2020.119](https://doi.org/10.1017/rdc.2020.119)
- Garcia N, Feranec RS, Passey BH, Cerling TE, Arsuaga JL. 2015. Exploring the potential of laser

- ablation carbon isotope analysis for examining ecology during the Ontogeny of Middle Pleistocene hominins from Sima de los Huesos (northern Spain). *PLOS ONE* 10:e0142895. doi: [10.1371/journal.pone.0142895](https://doi.org/10.1371/journal.pone.0142895)
- Gaudinski JB, Dawson TE, Quideau S, Schuur EAG, Roden JS, Trumbore SE, et al. 2005. Comparative analysis of cellulose preparation techniques for use with ^{13}C , ^{14}C , and ^{18}O isotopic measurements. *Analytical Chemistry* 77(22): 7212–7224. doi: [10.1021/ac050548u](https://doi.org/10.1021/ac050548u)
- Heinemeier J, Jungner H, Lindroos A, Ringbom Å, von Konow T, Rud N. 1997. AMS C-14 dating of lime mortar. *Nuclear Instruments & Methods in Physics Research B* 123(1–4):487–495.
- Heinemeier J, Ringbom Å, Lindroos A, Sveinbjornsdottir AE. 2010. Successful AMS C-14 dating of non-hydraulic lime mortars from the medieval churches of the Åland Islands, Finland. *Radiocarbon* 52(1):171–204.
- Hendriks L, Hajdas I, Ferreira E, Scherrer N, Zumbühl S, Küffner M, et al. 2019. Selective dating of paint components: radiocarbon dating of lead white pigment. *Radiocarbon* 61(2):473–493.
- Hendriks L, Caseri W, Ferreira SB, Scherrer NC, Zumbühl S, Küffner M, Hajdas I, Wacker L, Synal H-A, Gunther D. 2020a. The ins and outs of ^{14}C dating lead white paint for artworks application. *Analytical Chemistry* 92(11): 7674–7682. doi: [10.1021/acs.analchem.0c00530](https://doi.org/10.1021/acs.analchem.0c00530)
- Hendriks L, Kradolfer S, Lombardo T, Hubert V, Küffner M, Khandekar N, Hajdas I, Synal H., Hattendorf B, Günther D. 2020b. Dual isotope system analysis of lead white in artworks. *The Analyst* 145(4):1310–1318. Doi: [10.1039/C9AN02346A](https://doi.org/10.1039/C9AN02346A)
- Jones T, Levchenko V, King P, Troitzsch U, Wesley D, Williams A, Nayingull A. 2017. radiocarbon age constraints for a Pleistocene–Holocene transition rock art style: the northern running figures of the east Alligator River region, western Arnhem Land, Australia. *Journal of Archaeological Science Reports* 11:80–89. doi: [10.1016/j.jasrep.2016.11.016](https://doi.org/10.1016/j.jasrep.2016.11.016).
- Labeyrie J, Delibrias G. 1964. Dating of old mortars by carbon-14 method. *Nature* 201(492):742.
- Leavitt SW, Danzer SR. 1993. Method for batch processing small wood samples to holocellulose for stable-carbon isotope analysis. *Analytical Chemistry* 65(1):87–89. doi: [10.1021/ac00049a017](https://doi.org/10.1021/ac00049a017)
- Leroy S, L'Héritier M, Delqué-Kolic E, Dumoulin J-P, Moreau C, Dillmann P. 2015. Consolidation or initial design? Radiocarbon dating of ancient iron alloys sheds light on the reinforcements of French Gothic Cathedrals. *Journal of Archaeological Science* 53:190–201 doi: [10.1016/j.jas.2014.10.016](https://doi.org/10.1016/j.jas.2014.10.016)
- Leroy S, Delqué-Količ E, Vincent B, Baptiste P, Vega E, McGill F, et al. 2021. Le fer comme moyen de datation des bronzes khmers : première approche de prélèvement in situ. *Technè. La science au service de l'histoire de l'art et de la préservation des biens culturels* 82–91. doi:[10.4000/techn.10073](https://doi.org/10.4000/techn.10073)
- Lindroos A, Regev L, Oinonen M, Ringbom Å, Heinemeier J. 2012. C-14 dating of fire damaged mortars from medieval Finland. *Radiocarbon* 54(3–4):915–931.
- Message C et al. 2019. Datation par la méthode du radiocarbone de peintures au blanc de plomb apposées sur des cuirs dorés. In *Proceedings of the 11th Interim Meeting of the ICOM-CC Leather and Related Materials Working Group*. Publisher ICOM-CC. ISBN 978-2-491997-06-9.
- Message C, Beck L, de Viguerie L, Jaber M. 2020. Thermal analysis of carbonate pigments and linseed oil to optimize CO_2 extraction for radiocarbon dating of lead white paintings. *Microchemical Journal* 154:104637. doi: [10.1016/j.microc.2020.104637](https://doi.org/10.1016/j.microc.2020.104637)
- Message C, Beck L, Blamart D, Richard P, Germain T, Batur K, Gonzalez V, Foy E. 2022. 25 centuries of lead white manufacturing processes identified by ^{13}C and ^{14}C carbon isotopes. *Journal of Archaeological Science: Reports* 46. doi: [10.1016/j.jasrep.2022.103685](https://doi.org/10.1016/j.jasrep.2022.103685).
- Message C, Beck L, Germain T, Degryngny C, Serneels V, et al. 2021. Datation par la méthode du radiocarbone du blanc de plomb: du psimythion des cosmétiques antiques au pigment des peintures murales médiévales. *Technè* 52:102–110. doi: [10.4000/techn.10190](https://doi.org/10.4000/techn.10190).
- Moreau C, Message C, Berthier B, Hain S, Thellier B, Dumoulin J-P, et al. 2020. ARTEMIS, the ^{14}C AMS facility of the LMC14 national laboratory: a status report on quality control and microsample procedures. *Radiocarbon*. doi: [10.1017/RDC.2020.73](https://doi.org/10.1017/RDC.2020.73)
- Moreau C, Dumoulin J-P, Jaber M, Caffy I, Delqué-Količ E, Goulas C, Hain S, Perron M, Setti V, Sieudat M, et al. Forthcoming. Development of a ^{14}C protocol at the LMC14 for the dating of cultural heritage materials: historical mortars. Participation in the MODIS international intercomparison campaign. *Radiocarbon*. doi: [10.1017/RDC.2023.118](https://doi.org/10.1017/RDC.2023.118)
- Němec M, Wacker L, Hajdas I, Gäggeler H. 2010. Alternative methods for cellulose preparation for AMS measurement. *Radiocarbon* 52(3):1358–1370. doi: [10.1017/s0033822200046440](https://doi.org/10.1017/s0033822200046440)
- Quiles A, Emerit S, Asensi-Amorós V, Beck L, Caffy I, Delque-Količ E, Guichard H. 2021. New chronometric insights into Ancient Egyptian musical instruments held at the musée du Louvre and the musée des beaux-arts de Lyon. *Radiocarbon* 63(2):545–574. doi: [10.1017/RDC.2020.135](https://doi.org/10.1017/RDC.2020.135)
- Reiche I, Beck L, Caffy I. 2021. New results with regard to the Flora bust controversy: radiocarbon dating suggests nineteenth century origin. *Sci. Rep.* 11:8249. doi: [10.1038/s41598-021-85505-x](https://doi.org/10.1038/s41598-021-85505-x)
- Ricci G, Secco M, Marzaioli F, Terrasi F, Passariello I, Addis A, et al. 2020. The Cannero Castle

- (Italy): development of radiocarbon dating methodologies in the framework of the layered double hydroxide mortars. *Radiocarbon* 62(3):617–631.
- Richard B, Quilès F, Carteret C, Brendel O. 2014. Infrared spectroscopy and multivariate analysis to appraise α -cellulose extracted from wood for stable carbon 88 isotope measurements. *Chemical Geology* 381:168–179. doi: [10.1016/j.chemgeo.2014.05.010](https://doi.org/10.1016/j.chemgeo.2014.05.010)
- Rinne KT, Boettger T, Loader NJ, Robertson I, Switsur VR, Waterhouse JS. 2005. On the purification of α -cellulose from resinous wood for stable isotope (H, C and O) analysis. *Chemical Geology* 222(1–2):75–82. doi: [10.1016/j.chemgeo.2005.06.010](https://doi.org/10.1016/j.chemgeo.2005.06.010)
- Rosenheim BE, Thorrold SR, Roberts ML. 2008. Accelerator mass spectrometry ^{14}C determination in CO_2 produced from laser decomposition of aragonite. *Rapid Commun. Mass. Spectrom.* 22:3443–3449. doi: [10.1002/rcm.3745](https://doi.org/10.1002/rcm.3745)
- Scott EM. 2003. The Fourth International Radiocarbon Intercomparison (FIRI). Section 10: summary and conclusions. *Radiocarbon* 45(2):285–290.
- Scott EM, Lindroos A, Barrett G, Boudin M, Hajdas I, Olsen J, Maspero F, Marzaioli F, Michaska, Moreau C, Sironic A, Pawelczyk F. Forthcoming. Results and findings from an international mortar dating intercomparison MODIS2. *Radiocarbon*.
- Scott EM, Naysmith P, Cook G. 2017. Should archaeologists care about ^{14}C intercomparisons? Why? A summary report on SIRI. *Radiocarbon* 59(5):1589–1596. doi: [10.1017/RDC.2017.12](https://doi.org/10.1017/RDC.2017.12)
- Scott EM, Naysmith P, Dunbar E. 2023. Preliminary results from the Glasgow International Radiocarbon Intercomparison (GIRI). *Radiocarbon*. doi: [10.1017/RDC.2023.64](https://doi.org/10.1017/RDC.2023.64)
- Stuiver M, Smith C. 1965. Radiocarbon dating of ancient mortar and plaster. Washington, DC.
- Watchman AL, Lessard RA, Jull AJT, Toolin LJ, Blake W. 1992. ^{14}C dating of laser-oxidized organics. *Radiocarbon* 35:331–333. doi: [10.1017/S0033822200014090](https://doi.org/10.1017/S0033822200014090)
- Wilson AT, Grinsted MJ. 1977. $^{12}\text{C}/^{13}\text{C}$ in cellulose and lignin as palaeothermometers. *Nature* 265(5590):133–135. doi: [10.1038/265133a0](https://doi.org/10.1038/265133a0)